

WORLDWIDE GEOGRAPHICAL DISTRIBUTION OF BLACK SIGATOKA FOR BANANA: PREDICTIONS BASED ON CLIMATE CHANGE MODELS

Waldir Cintra de Jesus Júnior^{1*}; Ranolfo Valadares Júnior¹; Roberto Avelino Cecílio¹; Willian Bucker Moraes¹; Francisco Xavier Ribeiro do Vale²; Fábio Ramos Alves¹; Pierce Anderson Paul³

¹UFES/CCA - Depto. de Produção Vegetal - Lab. de Fitopatologia, Alto Universitário, s/n. C.P. 16 - 29500-000 - Alegre, ES - Brasil.

²UFV/CCA - Depto. de Fitopatologia - 36570-000 - Viçosa, MG - Brasil.

³Ohio State University, Dept. of Plant Pathology - Wooster, Ohio - USA.

*Corresponding author <wcintra@yahoo.com>

ABSTRACT: Global climatic changes will potentially influence plant diseases and the efficacy of their management options. One of the most likely impacts of climate change will be felt by the geographical distribution of plant diseases. Black Sigatoka is considered the most damaging and costly disease of banana. The socio-economic impact of this disease has continued to increase as the pathogen reaches new areas and the disease becomes more difficult to be controlled. The objectives of this research were to compare the global geographical distribution of the disease based on maps elaborated using weather data representing: i) current and future periods (2020, 2050 and 2080), ii) Intergovernmental Panel on Climate Change scenarios A2 and B2, iii) predictions based on six different climate change models and the “multimodel ensemble” and, iv) individual months. The “multimodel ensemble” lead to a reduction in the variability of the simulations when compared to the results obtained using the individual models separately. The predictions suggested that, in the future, areas favorable for the development of the Black Sigatoka disease will decrease. This reduction will occur gradually and will be higher for the A2 than for the B2 scenario. Changes in the geographical distribution of the disease will occur from one month to another, with unfavorable areas becoming favorable and vice-versa. However, in spite of these changes, extensive areas will still continue to be favorable for the occurrence of Black Sigatoka.

Key words: *Mycosphaerella fijiensis*, *Musa* spp., global climate change

DISTRIBUIÇÃO GEOGRÁFICA DA SIGATOKA NEGRA DA BANANEIRA ESTIMADA POR MODELOS DE MUDANÇAS CLIMÁTICAS GLOBAIS

RESUMO: As mudanças climáticas poderão alterar as doenças de plantas e afetar a eficácia das medidas de manejo. Um dos prováveis impactos será na distribuição geográfica das doenças. A Sigatoka Negra é considerada a principal doença da cultura da banana em decorrência dos danos causados e aumento do custo de manejo. O impacto sócio-econômico da doença continua aumentando, uma vez que a doença tem atingido novas áreas de plantio, tornando o manejo mais difícil. Este trabalho tem por objetivos comparar a distribuição geográfica da doença por meio da elaboração de mapas nas seguintes situações: a) clima atual e futuro (2020, 2050 e 2080), b) cenários A2 e B2 do Painel Intergovernamental de Mudanças Climáticas, c) predito por seis diferentes modelos de mudanças climáticas e pela média dos mesmos e, d) entre meses. Haverá redução das áreas favoráveis à doença no futuro, sendo que tal redução será mais acentuada no cenário A2 do que no B2 e gradativa para as décadas de 2020, 2050 e 2080. Predições efetuadas com o uso da média dos dados estimados pelos modelos permitiram redução na variabilidade da simulação em comparação com a predição gerada por cada modelo individualmente. Alterações na distribuição geográfica da doença ocorrerão entre meses, de modo que áreas consideradas desfavoráveis tornar-se-ão favoráveis e vice-versa. Apesar disso, extensas áreas continuarão favoráveis ao desenvolvimento da Sigatoka Negra.

Palavras-chave: *Mycosphaerella fijiensis*, *Musa* spp., mudanças climáticas globais

INTRODUCTION

Global climate change (GCC) is a major topic of discussion within both scientific and political forums. The Intergovernmental Panel on Climate Change (IPCC) is responsible for assessing information relevant to climate change and summarizing this information for policymakers and the public. GCC predictions are based on four scenarios (A1, A2, B1 and B2) that describe greenhouse gas emissions from potential resource using patterns, technological innovations, and demographics (IPCC, 2001).

Projections of future climate are made by computer models called Climate Change Models considering future greenhouse gas emissions simulated by each one of the four scenarios (A1, A2, B1 and B2). These models simulate climatic processes at different temporal and spatial scales to predict future changes at climate variables like air temperature, rainfall and relative humidity, among others.

A2 scenario describes a very heterogeneous world. The underlying theme is self-reliance and preservation of local identities. Fertility patterns across regions converge very slowly, which results in continuously increasing global population. Economic development is primarily regionally oriented and per capita economic growth and technological changes are more fragmented and slower than in other storylines (IPCC, 2001). The B2 scenario describes a world in which emphasis is put on local solutions for economic, social, and environmental sustainability. It is a world with continuously increasing global population at a rate lower than A2, intermediate levels of economic development, and less rapid and more diverse technological change than in the B1 and A1 storylines. While the scenario is also oriented toward environmental protection and social equity, it focuses on local and regional levels (IPCC, 2001).

The nature and magnitude of GCC will potentially influence plant diseases and the efficacy of their management options, impacting the productivity and sustainability of agricultural systems (Chakraborty et al., 1998). According to Chakraborty et al. (2000) one of the most likely impacts of climate change will be felt in the geographical distribution of plant diseases, with possible changes in the relative importance and spectrum of diseases and the emergence of new disease complexes. Modeling studies are essential to predict these alterations (Bergot et al., 2004; Scherm, 2004; Bourgeois et al., 2004), however methodology to use GCC models data on the prediction of global warming impacts on plant diseases has not yet been fully developed and still presents some lacks, like the use of the "multimodel ensemble", as it will be shown latter in this report.

Many studies were performed focusing plant diseases and global change. Carter et al. (1996) simulated climate changes in Finland concluding that increase in temperature will extend cereal cultivation areas in 2050. Moreover, the increase in the CO₂ level probably will generate higher yield which will alter the geographical distribution of nematodes, extending to the north of the country with a higher number of nematode generation per year. In another study, the risk to the late blight of potato (*Phytophthora infestans*) was estimated to be higher over all areas at Finland. Similar results were observed in Europe for the nematodes *Xiphinema* spp. and *Longidorus* spp. (Boag et al., 1991) and for *Phytophthora cinnamomi* (Brasier & Scott, 1994; Brasier et al., 1996). On other hand, these studies have focused on extratropical pathosystems, indicating a strong need for such studies on tropical areas.

Black Sigatoka (BS) (*Mycosphaerella fijiensis* Morelet) is considered one of the most damaging and costly diseases of banana (Marín et al., 2003). The socio-economic impact of BS continues to increase as the pathogen reaches new areas. As bananas are cultivated in more than 100 countries throughout the world and the impact of BS has also increased as it becomes more difficult to be controlled (Marín et al., 2003), therefore the ability to assess worldwide geographical distribution of the worse disease of banana under climate change has practical implications on climatic zoning of the crop, establishment of agricultural government politics and adequate disease management.

The main objective of this research was to compare the monthly worldwide geographical distribution of BS at the current time and in the future (2020, 2050 and 2080 decades) using current climate data and six different GCC model predictions. A secondary objective was to compare the geographical distribution predicted by the use of each one of the six different climate change models with the one made by the use of "multimodel ensemble".

MATERIAL AND METHODS

Current climate data, average air temperature and air relative humidity, were used to elaborate maps of the geographical distribution of BS. Current climatic conditions were characterized based on information for the period between 1961 to 1990, available in a matrix format with cells of 10' on latitude ´ 10' on longitude (New et al., 2002).

Data representing predicted variations in temperature and relative humidity for each month in the future were obtained from the IPCC website (IPCC, 2007). Future temperature data were calculated using

predicted temperature variations obtained by six different climate change models: HadCM3 (Hadley Centre Coupled Model version 3), CSIRO-Mk2 (Commonwealth Scientific and Industrial Research Organization GCM mark 2), CCSR/NIES (Centre for Climate Research Studies Model), ECHAM4 (European Centre Hamburg Model version 4), CGCM2 (Canadian Global Coupled Model version 2) and GFDL-R30 (Geophysical Fluid Dynamics Laboratory, R-30 resolution model) (IPCC, 2007). Only the HadCM3 model considered future variations in relative humidity, the other models assumed that relative humidity would remain constant or would only vary slightly in the future.

The chosen future scenarios were A2 and B2, with focus on the decades (or time slices) of 2020 (which comprises the periods of 2010 to 2039), 2050 (periods between 2040 and 2069) and 2080 (periods between 2070 and 2099) (IPCC, 2001). A1 and B1 scenarios were not used due to the fact that some climate change models don't use them to predict future variations on climate.

Predicted variations made by each model had a different spatial resolution (HadCM3: $3.75^\circ \times 2.5^\circ$, CSIRO-Mk2b: $5.625^\circ \times 3.214^\circ$, CCSR/NIES: $5.625^\circ \times 5.625^\circ$, ECHAM4: $2.8125^\circ \times 2.8125^\circ$, CGCM2: $3.75^\circ \times 3.75^\circ$ and GFDL-R30: $3.7^\circ \times 2.2^\circ$), so that climate variation data were resampled using the geographic information system (GIS) Idrisi 32[®] to generate maps with final spatial resolution of 10' on latitude \times 10' on longitude. For each month, these maps were summed using Idrisi 32[®] (arithmetical operation), with the maps of current temperature and relative humidity to obtain future projections of these climatic variables.

There is no definitive consensus regarding which model is most appropriate for calculating values of the climatic variable for future scenarios (IPCC, 2007). So, maps of spatial distribution of BS were elaborated using the current climate and the following situations: i) Future air temperature estimated by each of the six climate change models and future relative humidity obtained from the HadCM3 model; ii) Future

air temperature as the arithmetical mean of temperatures estimated using the six individual models and future relative humidity obtained from the HadCM3 model ("multimodel ensemble"). The methodology of map producing used was adapted of that one proposed by Hamada et al. (2006).

Based on the overlapping of maps of monthly average temperature and relative humidity, considering current and future period (2020, 2050 and 2080) for both scenarios (A2 and B2), new maps of disease distribution were elaborated using classes defined based on available epidemiological data on the effects of air temperature and relative humidity on the development of Black Sigatoka on banana (Table 1) (Meredith et al., 1973; Stover, 1983; Jacome et al., 1991; Jacome & Schuh, 1992; Mouliom-Pefoura et al., 1996; Romero & Sutton, 1997).

RESULTS AND DISCUSSION

From the total of 516 maps elaborated using monthly projections for current and future decades (2020, 2050 and 2080) in scenarios A2 and B2, only the results for the "multimodel ensemble" model are here shown (Figures 1 to 7). Complete results for simulations based on the six different climate change models and the "multimodel ensemble" are presented in Tables 2 to 4.

The intervals used in this study to characterize classes of favorability to BS were adequate because the obtained maps considering the current climate (Figure 1) were in agreement with data available in the literature (Mourichon et al., 1997; Carlier et al., 2000; Ghini et al., 2007). The pathogen produces conidia and ascospores and both play roles in the spread of the disease. Conidia are formed under conditions of high humidity, especially if there is a film of free water on the leaves. Ascospore release requires the presence of a rain or dew film of water that the pseudothecia imbibe and which results in the forcible ejection of the ascospores through the leaf boundary layer, from

Table 1- Classes of favorability for Black Sigatoka development defined as a function of temperature and relative humidity intervals.

Favorability Classes	Description	Temperature intervals	Relative humidity intervals
		°C	%
1	Highly favorable	25 to 28	> 90
2	Favorable	25 to 28	80 to 90
3	Relatively favorable	20 to 25 or 28 to 35	> 80
4	Little favorable	20 to 35	70 to 80
5*	Unfavorable	< 20 or > 35	< 70

*Favorability class 5 is defined if when any interval (temperature or relative humidity) occurs. For example: if temperature is between 20–35°C and relative humidity is less than 70% the area is classified at class 5.

Table 2- World area (%) occupied by the classes of favorability for Black Sigatoka for each month at current date and 2020 (A2 and B2 scenarios) situations predicted by six climate change models and the multimodel ensemble.

Month	Class	Current	A2							B2						
			CC ¹	CG ²	CS ³	EC ⁴	GF ⁵	HC ⁶	AM	CC ¹	CG ²	CS ³	EC ⁴	GF ⁵	HC ⁶	AM
January	1	0.085	0.003	0.003	0.003	0.003	0.003	0.003	0.003	0.004	0.004	0.004	0.004	0.004	0.004	0.004
	2	4.658	3.715	3.665	3.744	3.606	3.687	3.414	3.740	4.211	4.280	4.294	3.855	4.237	4.025	4.283
	3	2.092	1.216	1.238	1.145	1.294	1.201	1.482	1.156	1.349	1.255	1.234	1.683	1.286	1.504	1.249
	4	6.482	7.692	7.607	7.645	7.677	7.502	7.650	7.614	7.411	7.340	7.370	7.412	7.359	7.349	7.370
	5	86.683	87.374	87.487	87.463	87.421	87.608	87.451	87.488	87.025	87.121	87.098	87.046	87.115	87.119	87.095
February	1	0.211	0.007	0.007	0.007	0.007	0.007	0.007	0.007	0.009	0.009	0.009	0.009	0.009	0.009	0.009
	2	4.590	4.412	4.384	4.472	4.291	4.369	4.291	4.430	4.359	4.371	4.362	4.061	4.276	4.194	4.357
	3	1.719	1.137	1.152	1.046	1.240	1.168	1.226	1.101	1.209	1.168	1.170	1.488	1.261	1.343	1.187
	4	7.413	8.128	8.125	8.099	8.117	8.081	8.050	8.112	7.828	7.820	7.818	7.826	7.767	7.761	7.809
	5	86.067	86.316	86.332	86.376	86.344	86.375	86.426	86.350	86.594	86.632	86.641	86.616	86.687	86.693	86.638
March	1	0.207	0.004	0.004	0.004	0.004	0.004	0.004	0.004	0.007	0.007	0.007	0.008	0.007	0.007	0.007
	2	4.666	4.149	4.228	4.261	4.013	4.222	3.720	4.193	4.377	4.465	4.435	3.952	4.458	4.130	4.361
	3	1.396	1.194	1.096	1.051	1.298	1.071	1.578	1.117	1.313	1.163	1.259	1.690	1.202	1.514	1.294
	4	8.274	8.909	8.881	8.899	8.850	8.931	8.844	8.888	8.495	8.459	8.538	8.487	8.475	8.451	8.493
	5	85.457	85.744	85.791	85.785	85.836	85.771	85.854	85.798	85.808	85.906	85.760	85.863	85.857	85.897	85.845
April	1	0.159	0.006	0.004	0.003	0.005	0.005	0.005	0.005	0.006	0.004	0.005	0.005	0.006	0.005	0.005
	2	4.733	3.873	3.925	3.929	3.561	3.945	3.501	3.887	3.955	4.042	4.057	3.483	4.103	3.750	3.995
	3	1.356	1.335	1.341	1.305	1.647	1.278	1.722	1.337	1.491	1.422	1.493	2.009	1.376	1.691	1.477
	4	8.502	8.547	8.565	8.614	8.486	8.515	8.580	8.548	8.337	8.336	8.484	8.375	8.384	8.335	8.372
	5	85.249	86.240	86.165	86.150	86.301	86.258	86.192	86.224	86.211	86.196	85.961	86.128	86.132	86.219	86.151
May	1	0.100	0.010	0.010	0.010	0.010	0.010	0.010	0.010	0.008	0.008	0.008	0.008	0.008	0.008	0.008
	2	4.810	4.002	4.032	4.031	3.735	3.953	3.692	3.976	3.967	4.072	3.976	3.569	4.023	3.591	3.926
	3	1.605	1.578	1.545	1.555	1.851	1.619	1.872	1.602	1.610	1.500	1.607	2.017	1.567	1.987	1.656
	4	8.664	8.280	8.320	8.267	8.256	8.190	8.167	8.246	8.274	8.251	8.300	8.213	8.226	8.187	8.250
	5	84.821	86.130	86.093	86.137	86.148	86.228	86.258	86.166	86.142	86.170	86.110	86.193	86.176	86.228	86.160
June	1	0.067	0.035	0.032	0.032	0.035	0.032	0.034	0.033	0.035	0.035	0.036	0.041	0.037	0.035	0.036
	2	4.806	4.316	4.390	4.390	3.906	4.252	4.173	4.299	4.391	4.461	4.517	4.032	4.457	4.289	4.393
	3	3.027	2.129	2.059	2.055	2.554	2.191	2.267	2.148	2.068	1.988	1.938	2.437	1.987	2.165	2.062
	4	7.416	7.328	7.424	7.243	7.381	7.257	7.286	7.332	7.465	7.393	7.407	7.400	7.384	7.365	7.408
	5	84.683	86.191	86.096	86.281	86.124	86.268	86.240	86.189	86.040	86.122	86.102	86.090	86.136	86.145	86.101
July	1	0.008	0.029	0.028	0.029	0.030	0.030	0.029	0.029	0.023	0.022	0.025	0.025	0.023	0.029	0.024
	2	4.489	4.037	3.989	4.228	3.878	4.044	4.167	4.096	4.099	4.072	4.223	4.101	4.301	4.269	4.215
	3	3.905	3.058	3.093	2.850	3.242	3.041	2.926	2.998	3.153	3.149	3.018	3.159	2.937	2.981	3.029
	4	9.603	9.692	9.860	9.910	10.184	10.055	9.830	9.898	10.649	9.879	9.991	10.177	10.173	10.083	10.008
	5	81.995	83.185	83.031	82.983	82.665	82.830	83.048	82.979	82.077	82.878	82.744	82.538	82.566	82.638	82.725
August	1	0.009	0.026	0.023	0.025	0.027	0.027	0.028	0.026	0.019	0.020	0.019	0.021	0.020	0.022	0.020
	2	4.949	3.887	3.858	4.127	3.779	3.994	3.924	4.032	3.918	4.209	4.317	4.139	4.208	4.155	4.283
	3	3.725	3.093	3.106	2.844	3.218	2.997	3.058	2.948	3.559	3.225	3.150	3.339	3.224	3.314	3.179
	4	9.718	10.503	10.242	10.520	10.894	10.630	10.569	10.537	10.189	9.583	10.024	10.129	10.041	9.946	9.955
	5	81.599	82.490	82.770	82.483	82.083	82.352	82.421	82.457	82.314	82.964	82.490	82.372	82.507	82.563	82.562
September	1	0.006	0.005	0.005	0.015	0.005	0.005	0.005	0.005	0.007	0.007	0.007	0.007	0.007	0.007	0.007
	2	4.794	3.007	3.018	1.082	2.908	2.999	2.993	3.050	3.028	3.124	3.227	2.939	3.091	2.988	3.106
	3	2.371	2.041	2.002	2.438	2.140	2.015	2.026	1.977	2.247	2.119	2.022	2.322	2.145	2.254	2.144
	4	9.142	10.243	10.017	7.688	10.220	10.021	10.104	10.089	10.545	10.221	10.476	10.493	10.254	10.393	10.368
	5	83.686	84.704	84.957	88.777	84.727	84.960	84.873	84.879	84.173	84.529	84.268	84.238	84.503	84.358	84.375

Continue...

Table 2 - Continuation.

	1	0.006	0.005	0.005	0.005	0.005	0.005	0.005	0.005	0.007	0.006	0.006	0.006	0.006	0.006	0.006
	2	4.523	2.492	2.540	2.527	2.318	2.396	2.361	2.451	2.687	2.797	2.787	2.427	2.778	2.453	2.717
October	3	1.496	1.017	0.938	0.954	1.180	1.103	1.133	1.039	1.173	1.021	1.055	1.418	1.041	1.371	1.112
	4	7.621	9.081	8.806	8.793	8.907	9.065	9.021	8.922	8.643	8.340	8.390	8.485	8.325	8.417	8.429
	5	86.354	87.404	87.711	87.721	87.590	87.431	87.480	87.583	87.489	87.836	87.762	87.664	87.849	87.752	87.736
	1	0.022	0.005	0.005	0.005	0.005	0.005	0.005	0.005	0.006	0.006	0.006	0.006	0.006	0.006	0.006
	2	4.112	2.984	3.080	2.982	2.634	2.961	2.470	2.904	3.072	3.494	3.389	2.683	3.310	2.738	3.210
November	3	1.516	1.358	1.223	1.340	1.707	1.363	1.867	1.425	1.684	1.231	1.345	2.079	1.418	2.004	1.533
	4	7.375	8.108	7.904	8.010	8.002	7.995	8.045	8.011	7.768	7.597	7.664	7.697	7.645	7.712	7.682
	5	86.975	87.545	87.788	87.664	87.653	87.676	87.613	87.655	87.470	87.672	87.597	87.534	87.621	87.541	87.570
	1	0.049	0.008	0.008	0.008	0.008	0.008	0.008	0.008	0.009	0.009	0.009	0.009	0.009	0.009	0.009
	2	4.269	3.494	3.473	3.484	3.228	3.430	2.988	3.412	3.319	3.438	3.410	3.190	3.385	2.924	3.339
December	3	1.795	1.052	1.014	1.014	1.270	1.060	1.500	1.084	1.276	1.073	1.135	1.382	1.150	1.599	1.198
	4	7.480	8.416	8.241	8.329	8.288	8.218	8.254	8.290	8.386	8.326	8.438	8.365	8.365	8.351	8.380
	5	86.407	87.030	87.264	87.165	87.206	87.284	87.251	87.205	87.010	87.155	87.008	87.056	87.091	87.118	87.075

¹CCSR/NIES (Centre for Climate Research Studies Model); ²CSIROMk2 (Commonwealth Scientific and Industrial Research Organization GCM mark 2); ³CGCM2 (Canadian Global Coupled Model version 2); ⁴ECHAM4 (European Centre Hamburg Model version 4); ⁵GFDL-R30 (Geophysical Fluid Dynamics Laboratory, R-30 resolution model); ⁶HadCM3 (Hadley Centre Coupled Model version 3); ⁷Multimodel ensemble.

Table 3 - World area (%) occupied by the classes of favorability for Black Sigatoka for each month at current date and 2050 (A2 and B2 scenarios) situations predicted by six climate change models and the multimodel ensemble.

Month	Class Current	A2							B2							
		CC ¹	CG ²	CS ³	EC ⁴	GF ⁵	HC ⁶	AM	CC ¹	CG ²	CS ³	EC ⁴	GF ⁵	HC ⁶	AM	
January	1	0.085	0.002	0.002	0.002	0.002	0.002	0.002	0.002	0.002	0.002	0.002	0.003	0.002	0.003	0.002
	2	4.658	1.991	2.180	2.100	1.594	2.046	1.565	1.929	2.435	2.698	2.484	1.879	2.521	2.123	2.439
	3	2.092	1.406	1.143	1.201	1.761	1.268	1.763	1.405	1.534	1.221	1.411	2.040	1.355	1.774	1.475
	4	6.482	8.440	8.188	8.198	8.300	8.197	8.276	8.271	8.333	8.157	8.142	8.156	8.083	8.102	8.163
	5	86.683	88.161	88.488	88.500	88.344	88.487	88.394	88.393	87.695	87.921	87.960	87.923	88.038	87.998	87.920
February	1	0.211	0.009	0.011	0.011	0.008	0.011	0.009	0.011	0.007	0.007	0.007	0.007	0.007	0.008	0.007
	2	4.590	2.105	2.401	2.398	1.717	2.469	1.488	2.041	3.088	3.326	3.122	2.229	3.193	2.207	2.887
	3	1.719	1.723	1.421	1.385	2.089	1.357	2.321	1.771	1.704	1.431	1.623	2.532	1.542	2.531	1.868
	4	7.413	8.517	8.470	8.443	8.456	8.504	8.434	8.490	8.076	8.012	8.018	8.026	7.974	7.962	8.029
	5	86.067	87.647	87.697	87.763	87.730	87.660	87.748	87.688	87.124	87.224	87.230	87.206	87.285	87.293	87.209
March	1	0.207	0.015	0.018	0.018	0.010	0.018	0.017	0.017	0.009	0.008	0.008	0.008	0.008	0.008	0.008
	2	4.666	2.104	2.326	2.296	1.550	2.378	1.356	2.037	2.985	3.268	2.932	2.078	3.145	2.172	2.870
	3	1.396	2.122	1.873	1.831	2.558	1.727	2.770	2.114	2.150	1.827	2.106	2.979	1.842	2.803	2.174
	4	8.274	9.419	9.428	9.320	9.270	9.312	9.300	9.339	9.090	8.996	9.036	9.001	8.986	8.938	9.008
	5	85.457	86.340	86.355	86.535	86.611	86.565	86.557	86.493	85.766	85.901	85.919	85.934	86.019	86.078	85.940
April	1	0.159	0.001	0.006	0.006	0.000	0.010	0.002	0.001	0.003	0.003	0.004	0.000	0.004	0.003	0.003
	2	4.733	1.240	1.816	1.758	0.961	1.773	1.075	1.319	2.051	2.697	2.428	1.484	2.358	1.790	2.077
	3	1.356	2.527	1.977	2.066	2.752	1.929	2.660	2.432	2.704	2.017	2.300	3.248	2.343	2.898	2.631
	4	8.502	8.690	8.726	8.873	8.453	8.583	8.719	8.656	8.908	8.738	8.875	8.686	8.774	8.699	8.774
	5	85.249	87.543	87.474	87.298	87.833	87.705	87.544	87.592	86.334	86.546	86.393	86.581	86.522	86.610	86.514
May	1	0.100	0.036	0.043	0.045	0.030	0.044	0.042	0.041	0.041	0.040	0.042	0.037	0.033	0.040	0.040
	2	4.810	1.473	1.964	1.964	1.471	1.706	1.268	1.631	2.216	2.979	2.627	2.122	2.502	2.032	2.431
	3	1.605	2.247	1.735	1.720	2.237	2.011	2.421	2.066	2.757	1.955	2.318	2.832	2.298	2.896	2.510
	4	8.664	8.591	8.420	8.360	8.382	8.381	8.350	8.431	8.454	8.124	8.259	8.223	8.117	8.064	8.202
	5	84.821	87.653	87.837	87.911	87.880	87.858	87.919	87.830	86.532	86.903	86.755	86.787	87.050	86.968	86.816

Continue...

Table 3 - Continuation.

June	1	0.067	0.057	0.065	0.064	0.062	0.063	0.061	0.063	0.051	0.043	0.044	0.042	0.043	0.043	0.044
	2	4.806	2.332	2.576	2.526	1.994	2.374	1.804	2.275	2.957	3.240	3.048	2.637	2.967	2.877	2.966
	3	3.027	2.330	2.050	2.100	2.655	2.252	2.829	2.361	2.537	2.210	2.420	2.855	2.486	2.581	2.504
	4	7.416	8.006	7.765	7.750	7.749	7.571	7.597	7.672	8.758	8.127	8.247	8.289	8.103	8.102	8.205
	5	84.683	87.276	87.544	87.560	87.540	87.741	87.709	87.629	85.697	86.380	86.241	86.177	86.401	86.397	86.281
July	1	0.008	0.047	0.053	0.051	0.050	0.051	0.046	0.049	0.069	0.107	0.059	0.071	0.059	0.084	0.070
	2	4.489	2.826	3.089	3.023	2.745	2.932	2.542	2.907	3.427	3.586	3.541	3.300	3.519	3.450	3.532
	3	3.905	2.864	2.547	2.624	2.934	2.696	3.123	2.751	3.204	2.930	3.069	3.333	3.065	3.132	3.067
	4	9.603	10.490	9.851	9.492	10.021	10.124	9.980	9.798	11.027	9.173	9.662	10.055	9.771	9.828	9.730
	5	81.995	83.773	84.460	84.810	84.250	84.197	84.309	84.496	82.274	84.204	83.670	83.241	83.586	83.506	83.602
August	1	0.009	0.040	0.042	0.041	0.037	0.043	0.038	0.041	0.029	0.030	0.029	0.027	0.029	0.028	0.029
	2	4.949	2.614	2.961	2.865	2.544	2.765	2.674	2.803	3.080	3.727	3.576	3.241	3.564	3.393	3.518
	3	3.725	3.147	2.749	2.848	3.199	2.951	3.093	2.935	3.594	2.880	3.066	3.431	3.062	3.282	3.133
	4	9.718	10.452	9.437	9.803	10.418	10.363	10.360	10.107	10.482	9.069	9.728	10.186	10.250	10.079	9.905
	5	81.599	83.747	84.811	84.443	83.803	83.878	83.835	84.115	82.814	84.294	83.601	83.114	83.094	83.218	83.415
September	1	0.006	0.012	0.012	0.010	0.009	0.009	0.010	0.010	0.010	0.010	0.009	0.007	0.009	0.009	0.009
	2	4.794	2.025	2.059	2.027	1.667	1.925	1.818	1.913	2.300	2.411	2.243	1.893	2.201	2.192	2.207
	3	2.371	2.037	1.945	1.967	2.359	2.075	2.192	2.101	2.069	1.889	2.073	2.447	2.111	2.125	2.119
	4	9.142	9.795	9.178	9.263	9.529	9.239	9.284	9.365	9.907	9.243	9.394	9.545	9.424	9.373	9.481
	5	83.686	86.131	86.807	86.733	86.436	86.752	86.696	86.610	85.715	86.447	86.281	86.108	86.254	86.302	86.184
October	1	0.006	0.004	0.005	0.005	0.004	0.005	0.005	0.004	0.005	0.006	0.005	0.004	0.005	0.005	0.005
	2	4.523	1.379	1.651	1.633	1.227	1.505	1.367	1.459	1.541	1.909	1.754	1.311	1.784	1.724	1.671
	3	1.496	1.664	1.326	1.351	1.782	1.480	1.635	1.547	1.669	1.211	1.411	1.883	1.343	1.411	1.488
	4	7.621	8.067	7.328	7.250	7.426	7.335	7.574	7.482	7.770	7.028	7.106	7.291	7.201	7.229	7.271
	5	86.354	88.885	89.690	89.761	89.560	89.675	89.419	89.508	89.014	89.846	89.724	89.511	89.666	89.630	89.565
November	1	0.022	0.005	0.005	0.009	0.005	0.005	0.012	0.005	0.006	0.007	0.007	0.006	0.007	0.007	0.006
	2	4.112	1.446	1.733	1.678	1.342	1.587	1.513	1.554	1.944	2.159	1.979	1.671	1.923	1.957	1.939
	3	1.516	1.604	1.288	1.355	1.702	1.455	1.521	1.489	1.595	1.352	1.544	1.867	1.599	1.562	1.586
	4	7.375	7.481	7.207	7.236	7.238	7.250	7.322	7.297	7.830	7.596	7.685	7.714	7.658	7.676	7.693
	5	86.975	89.464	89.767	89.722	89.713	89.703	89.632	89.655	88.625	88.887	88.786	88.742	88.813	88.798	88.775
December	1	0.049	0.007	0.007	0.007	0.007	0.007	0.009	0.007	0.009	0.009	0.009	0.009	0.008	0.009	0.009
	2	4.269	1.493	1.758	1.679	1.391	1.598	1.512	1.574	2.191	2.489	2.213	1.623	1.960	1.963	2.099
	3	1.795	1.556	1.233	1.341	1.648	1.416	1.503	1.448	1.514	1.134	1.456	2.052	1.702	1.670	1.561
	4	7.480	8.298	8.025	8.149	8.181	8.123	8.167	8.167	8.691	8.423	8.576	8.530	8.542	8.466	8.548
	5	86.407	88.646	88.977	88.823	88.773	88.856	88.809	88.804	87.596	87.945	87.746	87.786	87.788	87.893	87.783

¹CCSR/NIES (Centre for Climate Research Studies Model); ²CSIROMk2 (Commonwealth Scientific and Industrial Research Organization GCM mark 2); ³CGCM2 (Canadian Global Coupled Model version 2); ⁴ECHAM4 (European Centre Hamburg Model version 4); ⁵GFDL-R30 (Geophysical Fluid Dynamics Laboratory, R-30 resolution model); ⁶HadCM3 (Hadley Centre Coupled Model version 3); ⁷Multimodel ensemble.

Table 4 - World area (%) occupied by the classes of favorability for Black Sigatoka for each month at current date and 2080 (A2 and B2 scenarios) situations predicted by six climate change models and the multimodel ensemble.

Month	Class Current	A2							B2							
		CC ¹	CG ²	CS ³	EC ⁴	GF ⁵	HC ⁶	AM	CC ¹	CG ²	CS ³	EC ⁴	GF ⁵	HC ⁶	AM	
January	1	0.085	0.003	0.001	0.002	0.002	0.001	0.002	0.001	0.002	0.003	0.003	0.005	0.003	0.002	0.002
	2	4.658	0.603	0.738	0.770	0.601	0.821	0.816	0.772	0.965	1.463	1.182	1.034	1.091	1.243	1.544
	3	2.092	1.983	1.797	1.771	1.986	1.721	1.740	2.661	1.917	1.344	1.635	1.813	1.380	1.576	2.411
	4	6.482	8.138	7.809	7.800	7.910	7.786	7.868	8.636	8.244	7.818	7.890	7.946	7.580	7.848	8.338
	5	86.683	89.274	89.655	89.657	89.501	89.671	89.574	87.929	88.872	89.372	89.290	89.202	89.945	89.331	87.706

Continue...

Table 4 - Continuation.

	1	0.211	0.001	0.002	0.003	0.002	0.002	0.002	0.002	0.003	0.010	0.005	0.007	0.008	0.007	0.002
	2	4.590	0.508	0.689	0.683	0.535	0.811	0.690	0.705	0.949	1.467	1.120	0.921	1.065	1.109	1.572
February	3	1.719	2.155	1.946	1.897	2.058	1.767	1.884	3.187	2.219	1.636	1.973	2.165	1.460	1.962	3.220
	4	7.413	7.899	7.821	7.780	7.751	7.751	7.740	8.669	8.766	8.624	8.661	8.645	7.666	8.609	8.135
	5	86.067	89.437	89.541	89.637	89.654	89.669	89.684	87.437	88.063	88.263	88.241	88.262	89.800	88.312	87.070
	1	0.207	0.001	0.003	0.005	0.002	0.014	0.003	0.002	0.005	0.014	0.010	0.004	0.024	0.010	0.007
	2	4.666	0.509	0.658	0.638	0.500	0.708	0.630	0.648	0.783	1.288	1.028	0.779	0.955	1.001	1.306
March	3	1.396	2.369	2.213	2.186	2.306	2.078	2.187	3.639	2.718	2.173	2.416	2.652	1.778	2.388	3.843
	4	8.274	9.190	9.119	9.007	8.925	8.916	8.914	9.546	9.407	9.337	9.305	9.266	8.852	9.206	9.120
	5	85.457	87.931	88.007	88.163	88.267	88.284	88.266	86.165	87.087	87.188	87.242	87.299	88.390	87.395	85.724
	1	0.159	0.001	0.001	0.001	0.001	0.001	0.001	0.000	0.000	0.002	0.000	0.000	0.005	0.000	0.000
	2	4.733	0.364	0.596	0.590	0.450	0.614	0.552	0.568	0.645	1.296	0.958	0.707	0.927	0.820	0.952
April	3	1.356	2.761	2.585	2.580	2.627	2.492	2.566	3.351	3.229	2.556	2.893	3.016	2.126	2.942	3.849
	4	8.502	7.954	7.887	7.816	7.475	7.307	7.542	9.344	7.832	7.613	7.720	7.348	7.132	7.486	9.062
	5	85.249	88.920	88.932	89.013	89.447	89.586	89.340	86.737	88.294	88.533	88.429	88.930	89.810	88.753	86.136
	1	0.100	0.013	0.029	0.036	0.022	0.033	0.046	0.013	0.015	0.046	0.037	0.018	0.068	0.039	0.030
	2	4.810	0.327	0.567	0.578	0.481	0.529	0.530	0.602	0.635	1.499	1.134	0.843	0.952	0.868	1.205
May	3	1.605	2.697	2.448	2.415	2.538	2.473	2.460	3.209	2.870	1.937	2.324	2.626	1.996	2.573	3.797
	4	8.664	6.833	6.622	6.569	6.547	6.565	6.464	8.778	7.779	7.462	7.528	7.526	6.354	7.404	8.461
	5	84.821	90.131	90.334	90.402	90.412	90.400	90.499	87.398	88.701	89.055	88.978	88.986	90.630	89.116	86.508
	1	0.067	0.047	0.072	0.085	0.051	0.074	0.084	0.039	0.054	0.064	0.063	0.051	0.093	0.063	0.039
	2	4.806	0.645	0.950	0.964	0.776	0.882	0.809	1.049	1.163	2.028	1.707	1.260	1.405	1.266	1.859
June	3	3.027	3.051	2.715	2.653	2.887	2.722	2.787	3.687	3.018	2.078	2.413	2.880	2.143	2.838	3.664
	4	7.416	7.757	6.423	7.480	6.518	6.176	6.459	8.484	7.813	6.891	7.627	7.025	6.000	6.881	8.543
	5	84.683	88.499	89.839	88.818	89.769	90.146	89.861	86.741	87.952	88.939	88.189	88.785	90.359	88.952	85.896
	1	0.008	0.047	0.079	0.083	0.060	0.086	0.079	0.053	0.077	0.072	0.074	0.070	0.083	0.067	0.068
	2	4.489	1.082	1.827	1.654	1.380	1.622	1.386	1.737	2.146	2.819	2.557	2.338	2.134	2.243	2.993
July	3	3.905	3.702	2.868	3.099	3.448	3.128	3.379	4.066	3.468	2.682	2.995	3.251	2.540	3.314	3.677
	4	9.603	9.479	8.348	7.441	7.758	7.762	8.012	11.615	11.200	8.975	8.907	9.317	6.959	9.350	10.587
	5	81.995	85.690	86.878	87.723	87.354	87.402	87.144	82.529	83.109	85.452	85.468	85.024	88.284	85.026	82.674
	1	0.009	0.027	0.053	0.056	0.030	0.055	0.053	0.031	0.049	0.044	0.044	0.032	0.055	0.040	0.026
	2	4.949	1.039	1.718	1.652	1.264	1.526	1.434	1.811	2.293	2.781	2.480	2.196	2.033	2.397	3.061
August	3	3.725	4.216	3.152	3.302	3.756	3.438	3.526	4.104	3.492	2.841	3.194	3.522	2.833	3.306	3.658
	4	9.718	13.150	8.719	9.975	10.331	9.698	11.002	13.101	12.977	8.857	10.593	10.650	8.497	10.530	10.936
	5	81.599	81.569	86.358	85.014	84.618	85.283	83.986	80.954	81.190	85.478	83.689	83.600	86.582	83.726	82.319
	1	0.006	0.017	0.017	0.015	0.011	0.011	0.013	0.007	0.011	0.010	0.011	0.008	0.021	0.011	0.006
	2	4.794	0.681	1.016	1.082	0.841	0.997	1.023	1.053	1.499	1.779	1.587	1.331	1.347	1.544	1.739
September	3	2.371	2.924	2.481	2.438	2.708	2.506	2.518	3.068	2.504	2.130	2.340	2.625	2.124	2.382	2.621
	4	9.142	8.656	7.458	7.688	7.983	7.476	7.842	10.197	9.486	8.624	8.890	9.076	7.344	8.814	9.797
	5	83.686	87.722	89.029	88.777	88.457	89.010	88.604	85.676	86.500	87.457	87.171	86.960	89.163	87.249	85.837
	1	0.006	0.001	0.001	0.001	0.001	0.001	0.001	0.000	0.002	0.004	0.002	0.002	0.003	0.003	0.002
	2	4.523	0.380	0.708	0.707	0.503	0.664	0.624	0.660	0.786	1.351	1.094	0.883	1.063	1.070	1.077
October	3	1.496	2.438	2.046	2.056	2.252	2.079	2.145	2.411	2.184	1.517	1.843	2.038	1.623	1.874	2.149
	4	7.621	7.525	6.522	6.715	6.674	6.591	6.930	8.266	7.839	6.782	7.222	7.127	5.974	7.325	7.603
	5	86.354	89.656	90.724	90.522	90.570	90.665	90.300	88.662	89.189	90.347	89.838	89.950	91.337	89.729	89.168
	1	0.022	0.005	0.002	0.002	0.002	0.002	0.004	0.001	0.003	0.005	0.003	0.004	0.008	0.005	0.004
	2	4.112	0.514	0.847	0.875	0.721	0.862	0.833	0.857	1.061	1.459	1.245	1.115	1.193	1.230	1.519
November	3	1.516	2.298	1.942	1.917	2.060	1.928	1.940	2.222	1.986	1.557	1.786	1.914	1.566	1.790	2.033
	4	7.375	6.003	5.565	5.621	5.675	5.656	5.721	7.674	6.111	5.760	5.930	5.887	5.376	5.920	7.893
	5	86.975	91.181	91.644	91.585	91.542	91.552	91.501	89.246	90.839	91.219	91.036	91.082	91.857	91.054	88.551
	1	0.049	0.002	0.002	0.005	0.002	0.002	0.006	0.001	0.004	0.007	0.006	0.007	0.006	0.002	0.005
	2	4.269	0.667	0.870	0.898	0.758	0.892	0.909	0.865	1.020	1.487	1.228	1.108	1.071	1.246	1.425
December	3	1.795	2.166	1.942	1.912	2.069	1.926	1.904	2.218	1.991	1.437	1.753	1.877	1.717	1.723	2.291
	4	7.480	6.100	5.655	5.818	5.893	5.862	5.865	8.496	8.010	7.573	7.804	7.747	5.603	7.718	8.727
	5	86.407	91.064	91.532	91.367	91.278	91.317	91.317	88.419	88.974	89.495	89.209	89.261	91.603	89.311	87.552

¹CCSR/NIES (Centre for Climate Research Studies Model); ²CSIROMk2 (Commonwealth Scientific and Industrial Research Organization GCM mark 2); ³CGCM2 (Canadian Global Coupled Model version 2); ⁴ECHAM4 (European Centre Hamburg Model version 4); ⁵GFDL-R30 (Geophysical Fluid Dynamics Laboratory, R-30 resolution model); ⁶HadCM3 (Hadley Centre Coupled Model version 3); ⁷Multimodel ensemble.

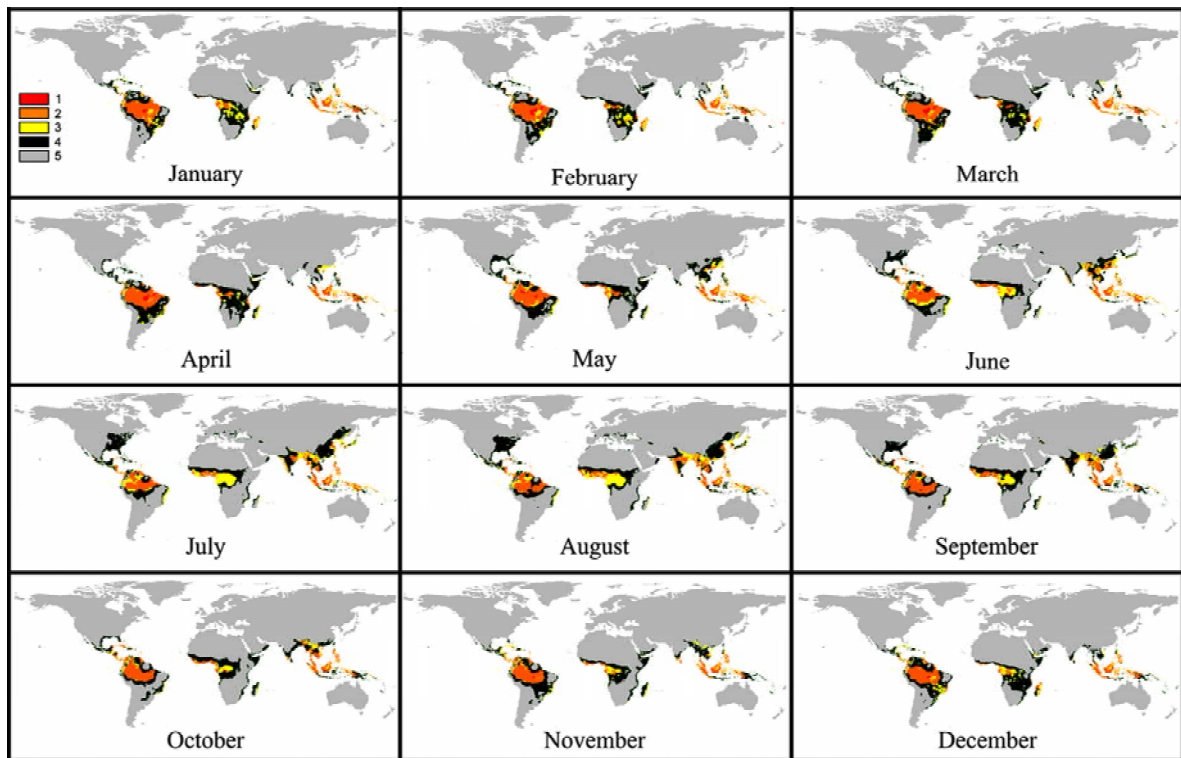


Figure 1- Maps representing current (1961-1990 average) worldwide spatial distribution of the classes of favorability for Black Sigatoka (BS) for January to December, where Class 1: highly favorable to BS; Class 2: favorable to BS; Class 3: relatively favorable to BS; Class 4: little favorable to BS and Class 5: unfavorable to BS.

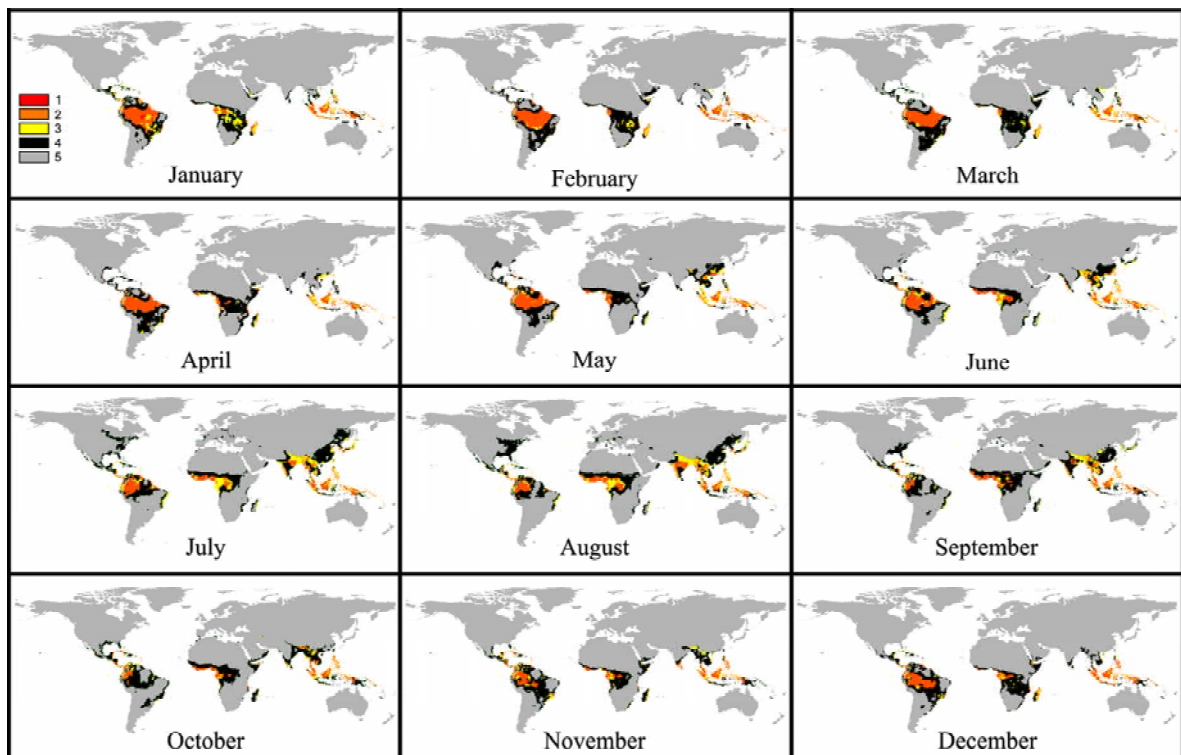


Figure 2 - Maps representing future worldwide spatial distribution of the classes of favorability for Black Sigatoka (BS), predicted by the use of the "multimodel ensemble", for the decade of 2020 (A2 scenario), where Class 1: highly favorable to BS; Class 2: favorable to BS; Class 3: relatively favorable to BS; Class 4: little favorable to BS and Class 5: unfavorable to BS.

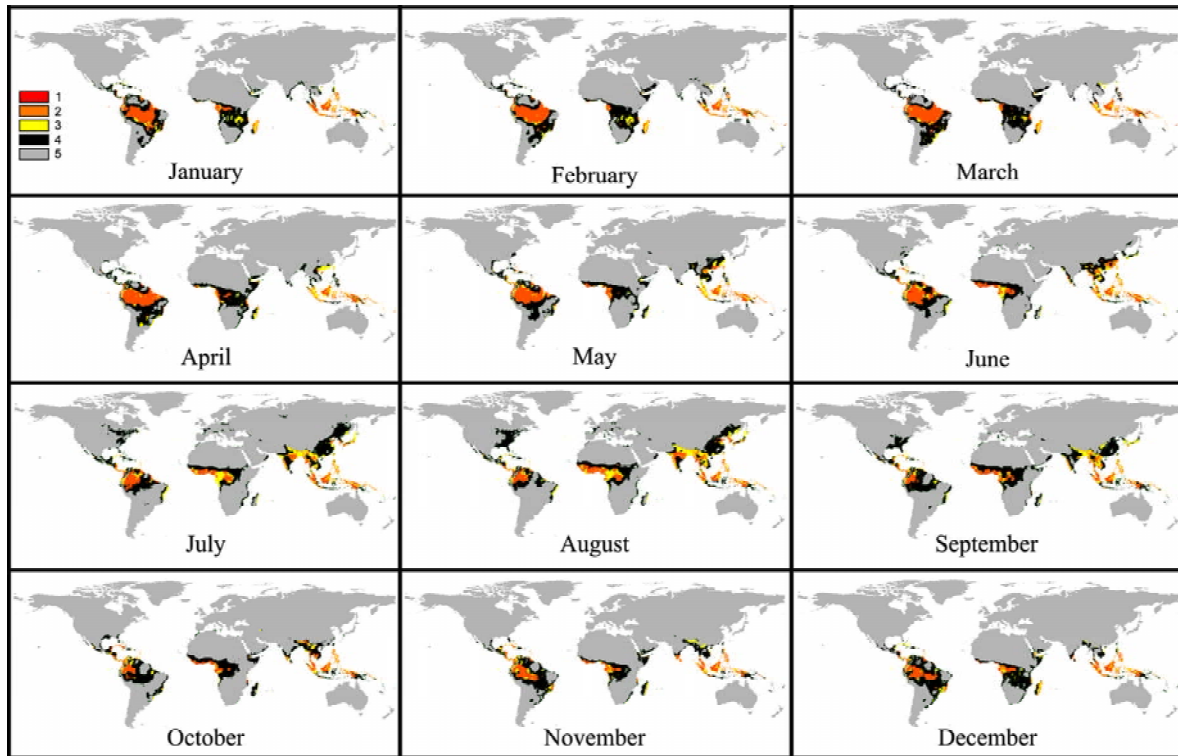


Figure 3 - Maps representing future worldwide spatial distribution of the classes of favorability for Black Sigatoka (BS), predicted by the use of the “multimodel ensemble”, for January to December, for the decade of 2020 (B2 scenario), where Class 1: highly favorable to BS; Class 2: favorable to BS; Class 3: relatively favorable to BS; Class 4: little favorable to BS and Class 5: unfavorable to BS.

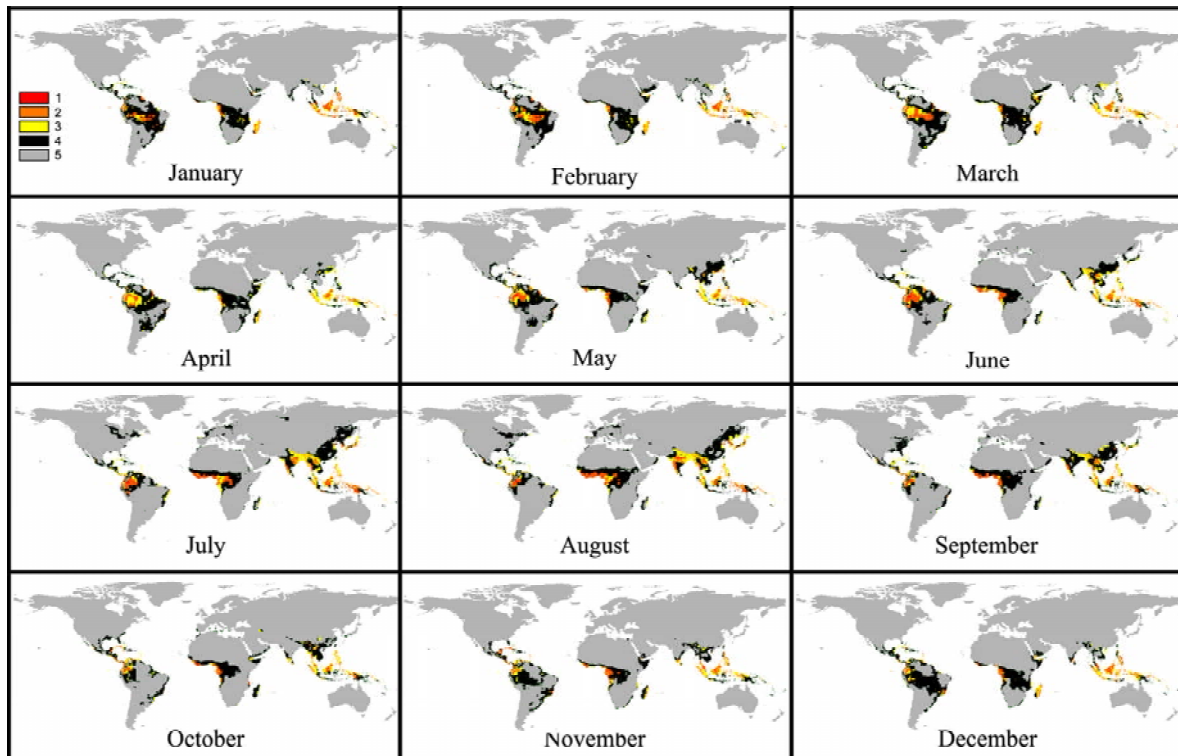


Figure 4 - Maps representing future worldwide spatial distribution of the classes of favorability for Black Sigatoka (BS), predicted by the use of the “multimodel ensemble”, for January to December, for the decade of 2050 (A2 scenario), where Class 1: highly favorable to BS; Class 2: favorable to BS; Class 3: relatively favorable to BS; Class 4: little favorable to BS and Class 5: unfavorable to BS.

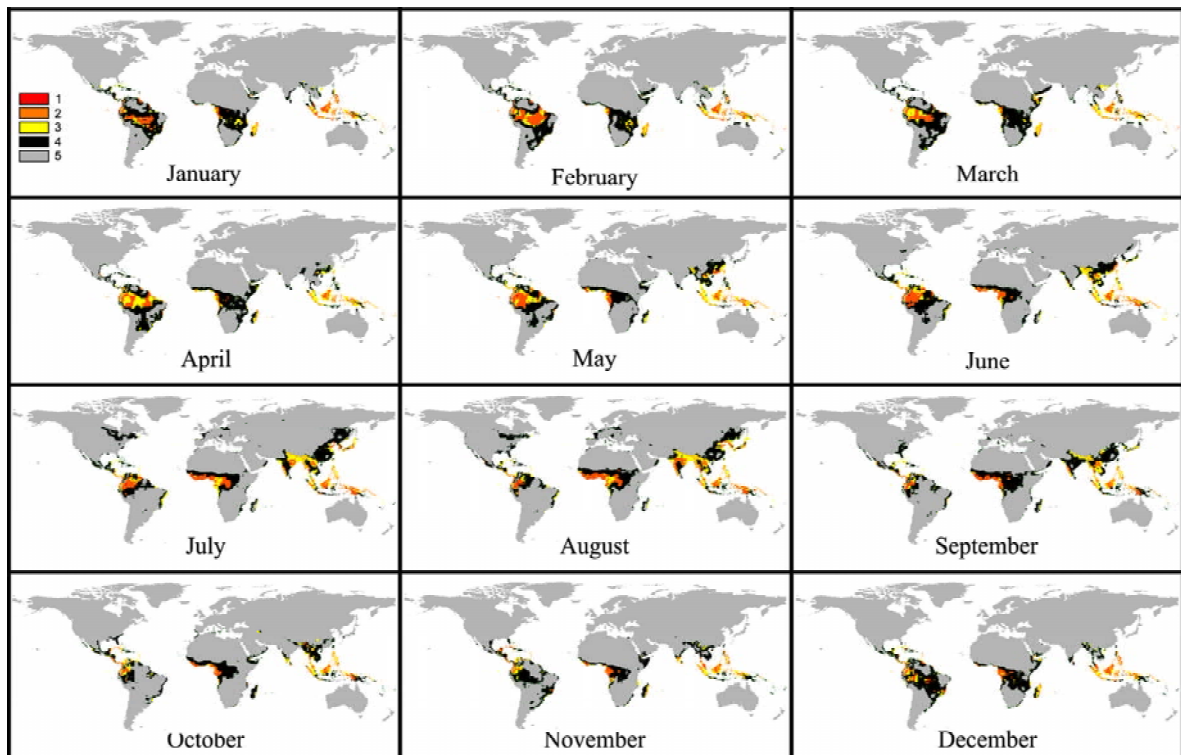


Figure 5 - Maps representing future worldwide spatial distribution of the classes of favorability for Black Sigatoka (BS), predicted by the use of the “multimodel ensemble”, for January to December, for the decade of 2050 (B2 scenario), where Class 1: highly favorable to BS; Class 2: favorable to BS; Class 3: relatively favorable to BS; Class 4: little favorable to BS and Class 5: unfavorable to BS.

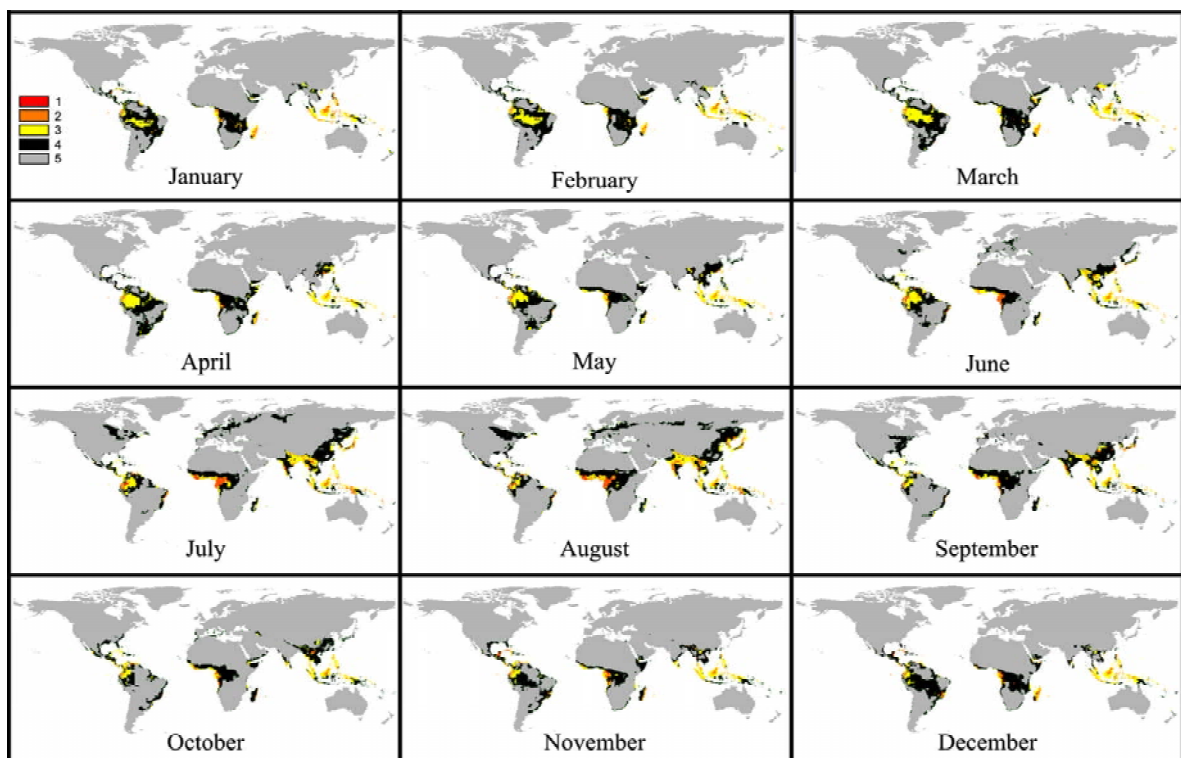


Figure 6 - Maps representing future worldwide spatial distribution of the classes of favorability for Black Sigatoka (BS), predicted by the use of the “multimodel ensemble”, for January to December, for the decade of 2080 (A2 scenario), where Class 1: highly favorable to BS; Class 2: favorable to BS; Class 3: relatively favorable to BS; Class 4: little favorable to BS and Class 5: unfavorable to BS.

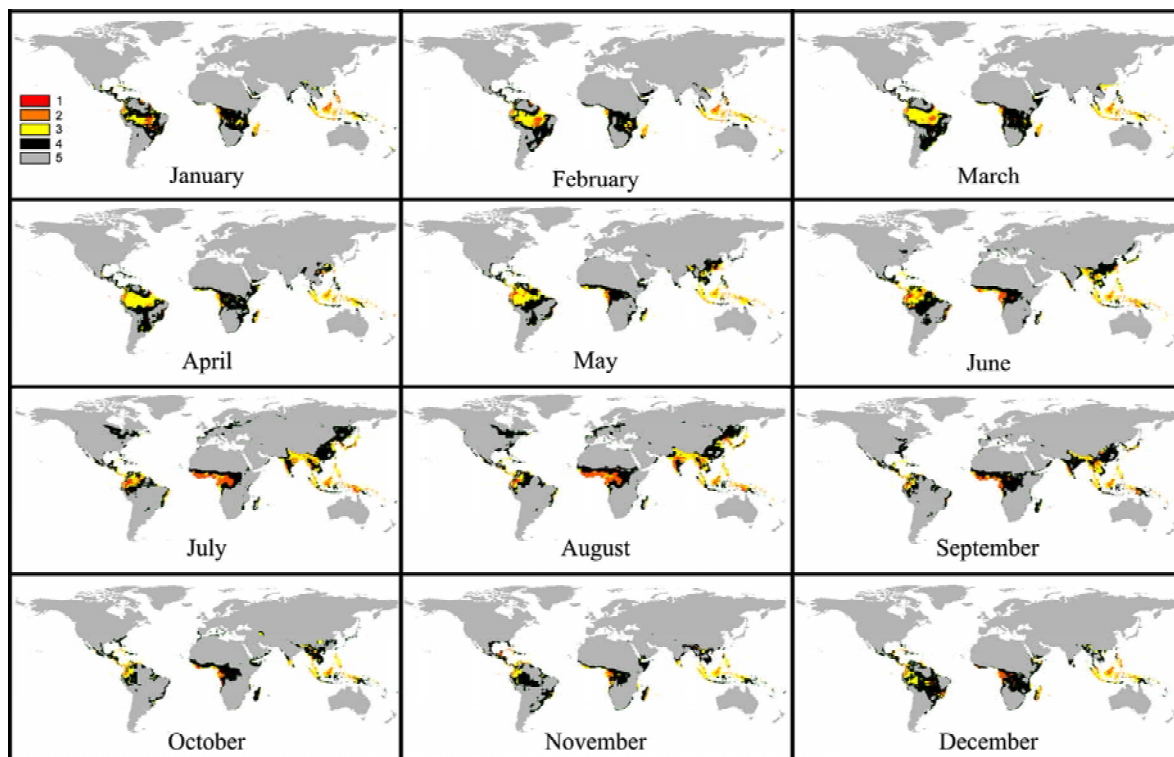


Figure 7 - Maps representing future worldwide spatial distribution of the classes of favorability for Black Sigatoka (BS), predicted by the use of the “multimodel ensemble”, for January to December, for the decade of 2080 (B2 scenario), where Class 1: highly favorable to BS; Class 2: favorable to BS; Class 3: relatively favorable to BS; Class 4: little favorable to BS and Class 5: unfavorable to BS.

where they are disseminated by air currents (Meredith et al., 1973). Conidia germinate over a wider range of relative humidity (92 to 100%) as compared to ascospores (98 to 100%). The effect of temperature on the germination can be characterized by a quadratic response function, with an estimated optimum at 26.5°C. Stover (1983) observed maximum growth of ascospore germ tubes at 26 to 28°C after 24 h incubation. The optimal temperature range for disease development was 25–28°C (Jacome et al., 1991; Jacome & Schuh, 1992).

Regarding the worldwide geographical distribution of the disease considering current and future periods, the results suggested that for both scenarios (A2 and B2) there will be a decrease in areas classified as 1 (highly favorable), 2 (favorable) and 3 (relatively favorable) and an increase of areas classified at 4 (little favorable) and 5 (unfavorable) (Figures 1 to 7) (Tables 2 to 4). These changes will be gradual for the decades of 2020, 2050 and 2080, with some exceptions that will be presented later in this paper. Results are in agreement with Ghini et al. (2007) who predicted that there will be a reduction of the favorable area to BS in Brazil in the future. Other authors also showed changes on the spatial distribution of favorability classes for other pathosystems in the fu-

ture, like Carter et al. (1996), Boag et al. (1991), Brasier & Scott (1994) and Brasier et al. (1996).

Variation in the worldwide geographical distribution of the disease will be higher for the A2 scenario as compared to B2, and will be different for the decades of 2020, 2050 and 2080 (Figures 1 to 7 and Tables 2 to 4). These findings are consistent with those of Ghini et al. (2007) on the probable impacts of climatic changes on BS in Brazil. The authors concluded that there will be a reduction in the favorable area to the disease in the Brazil and that the reduction will be higher for A2 scenario than for B2.

Some exceptions were detected, for example classes 3 and 4 in 2080. For class 3, an increase was observed in the area occupied by the same for scenario A2, which probably is related to the fact that some world areas that are not so warm (e.g. subtropical areas) will become favorable to the disease with an increase in temperature, especially when considering the interval between 20–25°C.

In the case of class 4, a decrease was also observed in the area represented by the same for the A2 scenario in 2080 which could be explained by a greater decrease in relative humidity for this decade. Gauhl (1994) reported that there is a reduction in the production of inoculum of *M. fijiensis* during drier (or

less rainy) months of the year in the Caribbean zone of Costa Rica, which is also the season with the lowest temperature. Others studies pointed out that successful infection is promoted by extended periods of high humidity and the presence of free water on leaves (Mayorga, 1990; Fullerton, 1994).

Analysis of the geographical distribution of the disease among months showed that in the future there will be a displacement in the worldwide geographical distribution of BS (Figures 1 to 7) in which unfavorable areas could become favorable and vice-versa as a function of increases in temperature and/or decreases in relative humidity. Colder months in the southern hemisphere (June, July and August), which are considered less favorable for the disease development at the current climatic conditions, could become more favorable due to increases in temperature. On the other hand, months which presented higher temperatures in this hemisphere (November, December and January) could become unfavorable to BS because of the extreme increases in the temperature and/or decreases in relative humidity. A great reduction in the areas of classes 1 (highly favorable), 2 (favorable) and 3 (relatively favorable) in November and December in the southern hemisphere will probably occur. This reduction will likely be lower in June and July. Thus, favorability will probably be gradually displaced from November to May (current condition) to January to July, for the years 2020 to 2080.

On the other hand, no such displacement was evident in the northern hemisphere for the classes among months of the year, due to hemispheric asymmetries in climate change predictions. Months most likely favorable to disease development will continue to be May to October. Additionally, it was clear from the results that areas occupied by classes 1, 2, 3 and 4 of the aforementioned months will increase, particularly in Southeast Asia, India and center-east United States. Thus, conditions of favorability to BS will be displaced northward.

When we consider three main worldwide banana producers (FAO, 2007) it is possible to conclude that spatial distribution of Black Sigatoka will be different in each country. For example, in the case of Brazil a gradual reduction in the favorable area to BS probably will occur in the decades of 2020, 2050 and 2080. However, favorable areas to the disease will probably increase in India and China if IPCC scenarios remain consistent.

Information available in the literature could help us to explain differences that will occur with spatial distribution of BS in the future. Simulations carried out in this study showed that the class 4 of favorability to disease development in Brazil tends to increase. This

will be a function of a decrease in relative humidity which could increase incubation and latent periods (lower numbers of pathogen cycles per year). Thus, the importance of the disease will probably be lower. In India and China, the situation will be the inverse.

Disease development is strongly related to weather conditions and plant susceptibility. Under very favorable conditions in Costa Rica and with a susceptible host, incubation periods of *M. fijiensis* can be as short as 13 to 14 days, whereas during periods of unfavorable weather, the duration of the incubation period can extend up to 35 days (Marín et al., 2003). Similar reports exist for Nigeria on plantains (Mobambo et al., 1996). During the rainy season, the incubation period was 14 days but in the dry season 24 days. Differences in the latent period from December 1993 to May 1995 for the susceptible cultivar Grande Nine, which is widely used for the fresh banana market, were observed in Guapiles, Costa Rica (Marín et al., 2003). The latent period ranged from 25 days during the rainy season (June to December) to 70 days during the dry season at the same locality. When the weather is highly conducive for ascospore discharge and infection, many infections occur on the leaves. When infections are dense, they rapidly coalesce at a very early stage of development, accelerating the appearance of mature spots that are characterized by the presence of pseudothecia and ascospores (Fouré et al., 1984). Under these conditions, leaves are rapidly and severely damaged.

In a general way, the use of the “multimodel ensemble” allowed reduction in the variability of simulation compared with data estimated by each model individually (Tables 2 to 4). It is important to point out that the “multimodel ensemble” analysis was used with success in other studies (Bergot et al., 2004; Cerri et al., 2007; Ghini et al., 2007; Marengo, 2007), not only related to Black Sigatoka or plant diseases. The adopted methodology allows the comparison between results obtained by each model and by the average of all (“multimodel ensemble”). This comparison could be extremely useful to direct and help new researches about the use of climate change models on the spatial distribution of plant diseases.

However, some exceptions were observed, particularly in 2080, in which each model simulated a decrease in the area occupied by classes considered favorable for disease development while results generated by the use of the “multimodel ensemble” simulated an increase (Tables 2 to 4). For the A2 scenario in 2080, great variations in the way data were analyzed were observed particularly for classes 3 (January and July) and 4 (April, May, July, September, October, November and December). For the B2 scenario for the

same decade variations were detected for the results of classes 3 (January and June) and 4 (April and November). Thus, caution should be taken when using the “multimodel ensemble”. More studies are necessary to reduce these uncertainties.

Climate changes certainly will affect the development of the plant. For the current conditions, banana is cultivated in more than 100 countries throughout the world, however, in the future changes in weather conditions may result in some areas becoming unsuitable for banana cultivations, causing commercial changes. Such situation, however, can be prevented with genetic improvement. In the same way, the pathogen can suffer more selection pressure. Prediction of the effect of climate change on pathogens and plants is difficult and speculative because the magnitude and range of these changes is very uncertain (Boag et al., 1991; Hillier, 1993). Nevertheless, although speculative, published data has suggested potential problems that may exist under a modified climate (IPCC, 2007).

Most plant disease models use different weather variables and operate at different spatial and temporal scales than do the global climate models. Improvements in the methodology are necessary to realistically assess disease impacts at a global scale.

Experimental research on a diverse range of disease systems is necessary to improve comprehension of climate change impacts. Given the multitude of atmospheric and climatic factors, the possible change in scenarios and the number of disease systems, modeling approaches to impact assessment need to be strengthened. For instance, changes in both mean temperature and its variability are equally important in predicting the potential impact of climate change (Scherin & Bruggen, 1994). Given that climate change is a global issue, the focus needs to shift from paddock-based assessment on specific diseases to a more ecologically relevant spatial unit (Scherin et al., 2000) to consider climate with other associated changes in land use and vegetation cover (Luo et al., 1995), among others.

Results obtained in this study could help to answer two important questions: (i) could preventative measures delay or prevent further spread of the disease?; and (ii) are those countries threatened by the disease taking measures to prevent the entry of the pathogen?

ACKNOWLEDGEMENTS

To CNPq (project 473999/2006-4), and for first author's support also by CNPq (project 308596/2006-4).

REFERENCES

- BERGOT, M.; CLOPPET, E.; PÉRARNAUD, V.; DÉQUÉ, M.; MARÇAIS, B.; DESPREZ-LOUSTAU, M.L. Simulation of potential range expansion of oak disease caused by *Phytophthora cinnamomi* under climate change. **Global Change Biology**, v.10, p.1539-1552, 2004.
- BOAG, B.; CRAWFORD, J.W.; NEILSON, R. The effect of potential climatic changes on the geographical distribution of the plant-parasitic nematodes *Xiphinema* and *Longidorus* in Europe. **Nematologica**, v.37, p.312-323, 1991.
- BOURGEOIS, G.; BOURQUE, A.; DEAUDELIN, G. Modelling the impact of climate change on disease incidence: a bioclimatic challenge. **Canadian Journal of Plant Pathology**, v.26, p.284-290, 2004.
- BRASIER, C.M.; DREYER, E.; AUSSENAC, G. *Phytophthora cinnamomi* and oak decline in southern Europe. Environmental constraints including climate change. **Annales des Sciences Forestières**, v.53, p.347-358, 1996.
- BRASIER, C.M.; SCOTT, J.K. European oak declines and global warming: a theoretical assessment with special reference to the activity of *Phytophthora cinnamomi*. **Bulletin OEPP/EPPO Bulletin**, v.24, p.221-232, 1994.
- CARLIER, J.; FOURÉ, E.; GAUHL, F.; JONES, D.R.; LEPOIVRE, P.; MOURICHON, X.; PASBERG-GAUHL, C.; ROMERO, R.A. Black leaf streak. In: JONES, D.R. (Ed.) **Diseases of banana, abacá and enset**. Wallingford: CAB International, 2000. p.37-79.
- CARTER, T.R.; SAARIKKO, R.A.; NIEMI, K.J. Assessing the risks and uncertainties of regional crop potential under a changing climate in Finland. **Agricultural and Food Science in Finland**, v.5, p.329-350, 1996.
- CERRI, C.E.P.; SPAROVEK, G.; BERNOUX, M.; EASTERLING, W.E.; MELILLO, J.M.; CERRI, C.C. Tropical agriculture and global warming: impacts and mitigation options. **Scientia Agricola**, v.64, p.83-99, 2007.
- CHAKRABORTY, S.; TIEDEMANN, A.V.; TENG, P.S. Climate change: potential impact on plant diseases. **Environmental Pollution**, v.108, p.317-326, 2000.
- CHAKRABORTY, S.; MURRAY, G.M.; MAGAREY, P.A.; YONOW, T.; SIVASITHAMPARAM, K.; O'BRIEN, R.G.; CROFT, B.J.; BARBETTI, M.J.; OLD, K.M.; DUDZINSKI, M.J.; SUTHERST, R.W.; PENROSE, L.J.; ARCHER, C.; EMMETT, R.W. Potential impact of climate change on plant diseases of economic significance to Australia. **Australasian Plant Pathology**, v.27, p.15-35, 1998.
- FOOD AND AGRICULTURE ORGANIZATION - FAO. ProdSTAT. Available at: <http://faostat.fao.org>. Accessed 30 Jul. 2007.
- FOURÉ, E.; GRISONI, M.; ZURFLUH, R. Les cercosporiosis du bananier et leurs traitements. Comportement des variétés. Etude de la sensibilité variétale des bananiers et plantains B *Mycosphaerella fijiensis* Morelet et de quelques caractéristiques biologiques de la maladie de rales noires au Gabon. **Fruits**, v.39, p.365-377, 1984.
- FULLERTON, R.A. Sigatoka leaf diseases. In: PLOETZ, R.C.; ZENTMYER, G.A.; NISHIJINIA, W.T.; ROHRBACH, K.G.; OHR, H.D. (Ed.) **Compendium of tropical fruit diseases**. St Paul: American Phytopathological Society, 1994. p.12-14.
- GAUHL, F. **Epidemiology and ecology of Black Sigatoka (*Mycosphaerella fijiensis* Morelet) on plantain and banana (*Musa* spp.) in Costa Rica, Central America**. Montpellier: INIBAP, 1994. 120p.
- GHINI, R.; HAMADA, E.; GONÇALVES, R.R.V.; GASPAROTTO, L.; PEREIRA, J.C. Análise de risco das mudanças climáticas globais sobre a sigatoka-negra da bananeira no Brasil. **Fitopatologia Brasileira**, v.32, p.197-204, 2007.
- HAMADA, E.; GHINI, R.; GONÇALVES, R.R.V. Efeito da mudança climática sobre problemas fitossanitários de plantas: metodologia de elaboração de mapas. **Engenharia Ambiental**, v.3, p.73-85, 2006.

- HILLIER, S. Climate change impacts on British vegetation creating tomorrow's climate today. **NERC News**, v.26, p.27-29, 1993.
- IPCC. Climate change 2007: the physical science basis: summary for policymakers. Geneva: IPCC, 2007. 18p. Available at: <http://www.ipcc.ch/SPM2feb07.pdf>. Accessed 10 Jun. 2007.
- IPCC. Climate change 2001: the scientific basis: summary for policymakers. Geneva: IPCC, 2001. 20p. Available at: <http://www.ipcc.ch/pub/spm22-01.pdf>. Accessed 10 Jun. 2007.
- JACOME, L.H.; SCHUH, W. Effects of leaf wetness duration and temperature on development of black Sigatoka disease on banana infected by *Mycosphaerella fijiensis* var. *difformis*. **Phytopathology**, v.82, p.515-520, 1992.
- JACOME, L.H.; SCHUH, W.; STEVENSON, R.E. Effect of temperature and relative humidity on germination and germ tube development of *Mycosphaerella fijiensis* var. *difformis*. **Phytopathology**, v.12, p.1480-1485, 1991.
- LUO, Y.; TEBEEST, D.O.; TENG, P.S.; FABELLAR, N.G. Simulation studies on risk analysis of rice leaf blast epidemics associated with global climate change in several Asian countries. **Journal of Biogeography**, v.22, p.673-678, 1995.
- MAYORGA, M.H. La Raya negra (*Mycosphaerella fijiensis* Morelet) del plátano y del banano. I. Ciclo de vida del patógeno bajo las condiciones del Urabá. **Revista ICA**, v.25, p.69-77, 1990.
- MARENGO, J. Cenários de mudanças climáticas para o Brasil em 2100. **Ciência & Ambiente**, v.34, p.97-114, 2007.
- MARÍN, D.H.; ROMERO, R.A.; GUZMÁN, M.; SUTTON, T.B. Black Sigatoka: an increasing threat to banana cultivation. **Plant Disease**, v.87, p.208-222, 2003.
- MEREDITH, D.S.; LAWRENCE, J.S.; FIRMAN, I.D. Ascospore release and dispersal on black leaf streak disease of bananas (*Mycosphaerella fijiensis*). **Transactions of the British Mycological Society**, v.60, p.547-554, 1973.
- MOBAMBO, K.M.; GAUHL, F.; PASBERG-GAUHL, C.; ZUOFA, K. Season and plant age effects evaluation of plantain for response to Black Sigatoka disease. **Crop Protection**, v.15, p.609-614, 1996.
- MOULIOM-PEFOURA, A.; LASSOUDIÈRE, A.; FOKO, J.; FONTEM, D.A. Comparison of development of *Mycosphaerella fijiensis* and *Mycosphaerella musicola* on banana and plantain in various ecological zones in Cameroon. **Plant Disease**, v.80, p.950-954, 1996.
- MOURICHON, X.; CARLIER, J.; FOURÉ, J. **Sigatoka leaf spot diseases**. Montpellier: INIBAP, 1997. 4p. (Musa Disease Fact Sheet, 8).
- NEW, M.; LISTER, D.; HULME, M.; MAKIN, I. A high-resolution data set of surface climate over global land areas. **Climate Research**, v.21, p.1-25, 2002.
- ROMERO, R.A.; SUTTON, T.B. Reaction of four *Musa* genotypes at three temperatures to isolates of *Mycosphaerella fijiensis* from different geographical regions. **Plant Disease**, v.81, p.1139-1142, 1997.
- SCHERM, H. Climate change: can we predict the impacts on plant pathology and pest management? **Canadian Journal of Plant Pathology**, v.26, p.267-273, 2004.
- SCHERM, H.; SUTHERST, R.W.; HARRINGTON, R.; INGRAM, J.S.I. Global networking for assessment of impacts of global change on plant pests. **Environmental Pollution**, v.108, p.333-341, 2000.
- SCHERM, H.; BRUGGEN, A.H.C. van. Global warming and nonlinear growth: how important are changes in average temperature? **Phytopathology**, v.84, p.1380-1384, 1994.
- STOVER, R.H. The effect of temperature on ascospore germ tube growth of *Mycosphaerella musicola* and *Mycosphaerella fijiensis* var. *difformis*. **Fruits**, v.38, p.625-628, 1983.

Received November 01, 2007

Accepted June 12, 2008